Asymmetry of the Spin Reorientation Transition in Ultrathin Fe Films and Wedges Grown on Ag(100)

Z. Q. Qiu, J. Pearson, and S. D. Bader

Materials Science Division, Argonne National Laboratory, Argonne, Illinois 60439

(Received 24 August 1992)

Fe(100) films and wedge-shaped overlayers were grown epitaxially onto Ag(100) and investigated *in situ* by means of the surface magneto-optic Kerr effect. The reversible spin reorientation transition between perpendicular and in-plane alignment at T_R, which is below the Curie temperature T_C, is characterized for critical thicknesses d_R along the length of a wedge. A similar asymmetry is identified within pseudogap regions in the vicinity of both T_R and d_R in which the remanent magnetization is small but nonvanishing.

PACS numbers: 75.40.Cx, 05.70.Jk, 75.70.Ak

The broken translational symmetry in the perpendicular direction of an ultrathin magnetic film can induce a surface magnetic anisotropy which plays an important role in determining the magnetic properties of two-dimensional (2D) systems [1]. The surface anisotropy can even dominate the magnetic shape anisotropy to yield a spontaneous magnetization perpendicular to the film plane [2–4]. It is well known from the Mermin-Wagner theorem [5] that a 2D isotropic Heisenberg system does not have long-range magnetic order at finite temperature. However, the surface magnetic anisotropy can stabilize long-range order and make the system Ising-like [6]. The interesting question is what will happen when the surface anisotropy just compensates the shape anisotropy? Theoretical studies [1,7] suggest that there exists a temperature below the Curie temperature T_C at which the magnetization switches from perpendicular to in-plane, and that in the vicinity of this spin reorientation transition temperature T_R there is a region in temperature ΔT_R wherein the long-range magnetic order is lost [1]. Pappas and co-workers investigated the Fe/Cu(100) [8] and Fe/Ag(100) [9] systems by means of spin-polarized secondary-electron spectroscopy and, indeed, reported the existence of such a temperature, but their value of ΔT_R was an order of magnitude larger than predicted [1]. We reinvestigate the Fe/Ag(100) system herein by means of the surface magneto-optic Kerr effect (SMOKE). Our sensitivity permits us to identify previously undetected asymmetric structure with pseudogap regions defined by ΔT and Δd within which the remanent magnetization is greatly suppressed but nonvanishing.

Fe/Ag(100) has been studied extensively in the past decade. Although the growth of Fe on Ag(100) is still controversial [10,11], the perpendicular easy axes of magnetization in the ultrathin regime are now well established [2,12]. Our Ag(100) single-crystal substrate was prepared by mechanical polishing down to a 0.25-μm diamond-paste finish, followed by chemical polishing using the method of Lam, Rothman, and Nowicki [13]. Then the substrate was ultrasonically cleaned in methanol before its introduction into the ultrahigh vacuum (UHV) chamber of base pressure 3×10^{-10} Torr. The experimental system was illustrated previously [14,15]. After cycles of 3-keV Ar-ion sputtering and annealing at 700 °C for half hour intervals to clean the Ag substrate, a well-defined Ag(100) surface was formed, as indicated by the reflection high-energy electron diffraction (RHEED) and low-energy electron diffraction (LEED) patterns

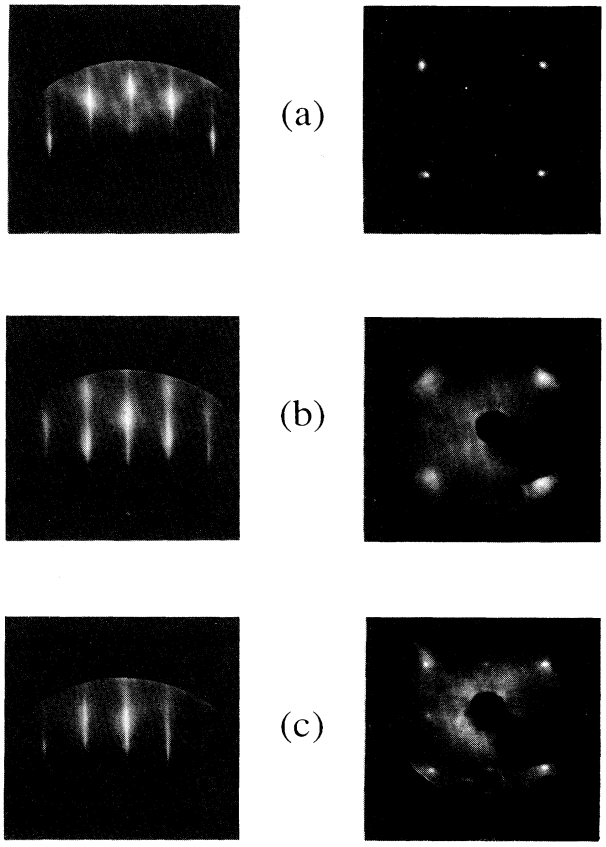

FIG. 1. The RHEED (left) and LEED (right) patterns for (a) the Ag(100) substrate; (b) 6 ML of Fe on Ag(100); and (c) after annealing of the film in (b) at 150 °C. The electron energy of the LEED pictures is −120 eV.

[Fig. 1(a)].

The Fe film was grown onto the Ag(100) substrate at room temperature. The evaporation rate was monitored by a quartz thickness monitor and was typically ~ 0.6 Å/min. After the Fe deposition the film was annealed at 150 °C for half an hour. The RHEED and LEED patterns of a 6-ML (monolayer) Fe film before and after annealing are shown in Figs. 1(b) and 1(c), respectively. It is obvious that single-crystalline Fe(100) has formed, and that the anneal smoothed the Fe film as indicated by the sharpening of the RHEED and LEED beams. The Fe films were grown into wedged shapes (with slopes of 0.2–0.5 ML/mm) with the gradient along the [001]. The method used to create the wedges was the same as described earlier [15]. The advantage of wedged samples is their continuous change of film thickness, as has been appreciated recently in the study of coupled magnetic multilayers [15,16].

The magnetic properties of the films were investigated *in situ* by means of SMOKE measurements with the external magnetic field either perpendicular (polar) or parallel (longitudinal) to the film plane [17]. The laser beam was focused to a spot size of ~ 0.2 mm onto the sample. Thus, the thickness variation probed due to the wedge shape is only ~ 0.04–0.1 ML within the laser spot; so the thickness within the laser spot is virtually uniform. We confirm that the easy axes of magnetization at room temperature for films less than ~ 7 ML of Fe are perpendicular to the film plane, as indicated by polar Kerr hysteresis loops with full remanence.

We first studied the reorientation transition by changing T for a 6-ML Fe overlayer. The results are shown in the Kerr loops of Fig. 2 in which the external magnetic field is applied either perpendicular to the film plane or in-plane, and labeled polar and longitudinal, respectively. The polar loops have full remanence and low coercivities ($H_c \sim 70$ Oe) for $T \leq 330$ K, and the remanent $M \rightarrow 0$ as T increases to 380 K. This indicates that the easy axes are perpendicular to the film plane for $T < 380$ K, while they are in the film plane above 380 K (as indicated by the zero remanence of the polar signal and the squareness of the longitudinal loops for $T \geq 380$ K). However, for $T < 380$ K the signals labeled longitudinal exhibit apparent coercivities and remanences that are significant in magnitude. In fact a longitudinal Kerr signal should only have $\sim 10^{-1}$ of the magnitude of the corresponding polar signal [17]. This suggests that the loops in question labeled longitudinal are dominated by perpendicular magnetization orientations even though the applied field is in-plane. The detailed shape of these loops is probably governed by a misalignment (estimated $\sim 7°$) of the field orientation relative to the film plane.

In order to understand the magnetic structure in detail, we plot the remanence of the perpendicular component ($M_\perp$) determined from the polar signal, and the remanence of the parallel component ($M_\parallel$) determined from the true longitudinal signal versus T in Fig. 3. The trends can be divided into five regions: (I) For $T < 330$ K, $M_\perp$ remains at its saturation value; (II) for 330 K $< T <$ 345 K, $M_\perp$ drops precipitously; (III) for 345 K $< T <$ 380 K, $M_\perp$ decreases gradually to approach zero; (IV) for 380 K $< T <$ 420 K, $M_\perp$ is zero and $M_\parallel$ increases abruptly from zero; and (V) for $T > 420$ K, $M_\parallel$ retains its saturation value. Regions II–IV encompass the reorientation transition. In region III, M is greatly suppressed from its saturation value. This region is similar to that observed in Fe/Cu(100) and Fe/Ag(100) by Pappas and coworkers [8,9]. But the significant difference is that M is not zero in our case in region III. Erickson and Mills [1] estimate that the width ΔT_R of their unstable region should be only $\sim 0.5\%$ of T_R, or ~ 1–2 K in the present case. The ΔT_R region in which there is no long-range or-

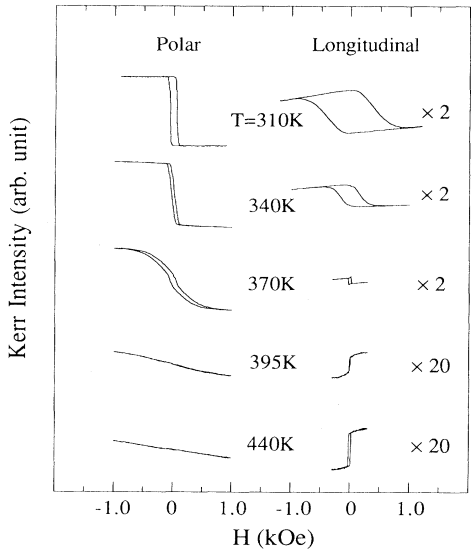

FIG. 2. The hysteresis loops for (left panel) perpendicular (polar) and (right panel) in-plane (labeled longitudinal) magnetic-field configurations for a 6.0-ML Fe film at different temperatures.

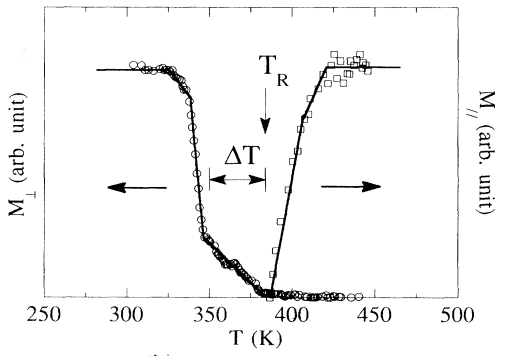

FIG. 3. The perpendicular and parallel components of the remanent magnetization for a 6.0-ML Fe film vs T.

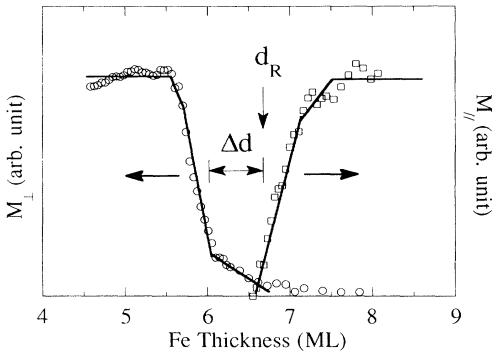

FIG. 4. The perpendicular and parallel components of the magnetization at room temperature for Fe films of different thickness along a wedge.

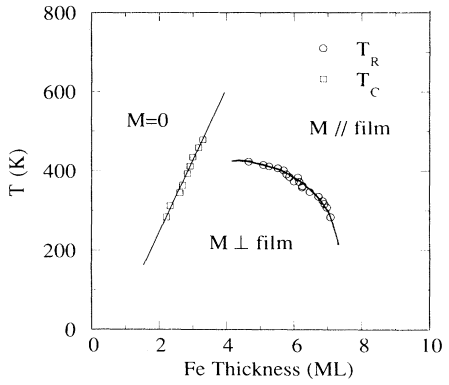

FIG. 5. Magnetic phase diagram of Fe/Ag(100).

der is ascribed within their theory to a spin excitation spectrum whose gap vanishes due to the establishment of isotropy. We identify our region III (and that of Pappas, Brundle, and Hopster [9] by implication) as *not* being associated with a loss of long-range order, but as a *pseudogap* ΔT which possesses complex magnetic structure. M exhibits asymmetric behavior within the pseudogap: $M_\parallel \rightarrow 0$ abruptly on the approach from $T > T_R$; but while $M_\perp$ initially drops abruptly, it then more gradually goes to zero on the approach from $T < T_R$. Our conclusions presumably differ from those of Pappas and coworkers [8,9] because we have enhanced sensitivity to observe the asymmetry within ΔT. If there is a region in which long-range order vanishes, it appears to be no larger in width than the 1–2 K estimate of Erickson and Mills. But why do those authors not predict the asymmetric structure that we observe? We suggest that it may be because their theoretical model is based on a 2D lattice which does not include cubic bulk magnetic anisotropy. In the actual Fe/Ag(100) system, however, the Fe film of interest is of finite thickness and the cubic bulk anisotropy should start to manifest itself, especially when the surface anisotropy cancels the shape anisotropy.

We also studied the reorientation transition as a function of the Fe film thickness. The remanence values $M_\parallel$ and $M_\perp$ at room temperature are plotted in Fig. 4 versus the Fe film thickness along a wedge. The hysteresis loops are similar to those observed in Fig. 2. Five thickness regions in the vicinity of the transition at d_R appear in Fig. 4, and these regions exhibit the same asymmetric character as those identified in Fig. 3. One of them (indicated by Δd in Fig. 4) defines the analogous pseudogap.

We construct a magnetic phase diagram in Fig. 5 to summarize our findings. For the purposes of characterizing the thickness dependence of T_C we used as the operational definition that T_C is the T *above which* all remanence vanishes. We define T_R as the $T < T_C$ *at which* the in-plane remanent magnetic component starts to develop. The T_C and T_R values thusly determined are shown in Fig. 5 for different thicknesses of Fe films along two wedged samples, respectively. As expected, T_R decreases as the Fe film thickness increases. Combined with the thickness dependence we determined for T_C, Fig. 5 represents a magnetic phase diagram that delineates the $M = 0$, $M_\parallel$, and $M_\perp$ phases.

In summary, wedge-shaped Fe films grown on an Ag(100) substrate were investigated via SMOKE measurements. The reorientation transition for the magnetization from perpendicular to in-plane was studied by both changing temperature and the thickness of the Fe film. In both cases, a pseudogap region is identified below T_C in which the remanent magnetization is greatly suppressed from its saturation value, and exhibits asymmetric behavior. But the magnetization is not truly zero within the pseudogap region. A magnetic phase diagram is constructed that delineates the $M = 0$, $M_\parallel$, and $M_\perp$ phases.

The work was supported by U.S. Department of Energy, Basic Energy Sciences–Materials Sciences, under Contract No. W-31-109-ENG-38.

[1] R. P. Erickson and D. L. Mills, Phys. Rev. B **46**, 861 (1992).
[2] U. Gradmann, J. Magn. Magn. Mater. **54-57**, 733 (1986).
[3] N. C. Koon, B. T. Jonker, F. A. Volkening, J. J. Krebs, and G. A. Prinz, Phys. Rev. Lett. **59**, 2463 (1987).
[4] C. Liu, E. R. Moog, and S. D. Bader, Phys. Rev. Lett. **60**, 2422 (1988); C. Liu and S. D. Bader, J. Appl. Phys. **67**, 5758 (1990).
[5] M. D. Mermin and H. Wagner, Phys. Rev. Lett. **17**, 1133 (1966).
[6] M. Bander and D. L. Mills, Phys. Rev. B **38**, 12015 (1988).
[7] D. Pecia and V. L. Pokrovsky, Phys. Rev. Lett. **65**, 2599 (1990).
[8] D. P. Pappas, K.-P. Kämper, and H. Hopster, Phys. Rev. Lett. **64**, 3179 (1990).
[9] D. P. Pappas, C. R. Brundle, and H. Hopster, Phys. Rev.

B **45**, 8169 (1992).

[10] W. F. Egelhoff, Jr. and I. Jacob, Phys. Rev. Lett. **62**, 921 (1989); B. Heinrich, Z. Celinski, J. F. Cochran, W. B. Muir, Q. M. Zhong, A. S. Arrott, and K. Myrtle, Phys. Rev. Lett. **64**, 673 (1990).

[11] H. Li, Y. S. Li, J. Quinn, D. Tian, J. Sokolov, F. Jona, and P. M. Marcus, Phys. Rev. B **42**, 9195 (1990).

[12] B. T. Jonker, K.-H. Walker, E. Kisker, G. A. Prinz, and C. Carbone, Phys. Rev. Lett. **57**, 142 (1986); B. Heinrich, K. B. Urquhart, A. S. Arrott, J. F. Cochran, K. Myrtle, and S. T. Purcell, Phys. Rev. Lett. **59**, 1756 (1987); M. Stampanoni, A. Vaterlaus, M. Aeschlimann, and F. Meier, Phys. Rev. Lett. **59**, 2483 (1987); J. Araya-Pochet, C. A. Ballentine, and J. L. Erskine, Phys. Rev. B **38**, 7846 (1988).

[13] N. Q. Lam, S. J. Rothman, and L. J. Nowicki, J. Electrochem. Soc. **119**, 715 (1972).

[14] Z. Q. Qiu, J. Pearson, and S. D. Bader, Phys. Rev. Lett. **67**, 1646 (1991).

[15] Z. Q. Qiu, J. Pearson, A. Berger, and S. D. Bader, Phys. Rev. Lett. **68**, 1398 (1992).

[16] J. Unguris, R. J. Celotta, and D. T. Pierce, Phys. Rev. Lett. **67**, 140 (1991); S. T. Purcell, W. Folkerts, M. T. Johnson, N. W. E. McGee, K. Jager, J. ann de Stegge, W. B. Zeper, W. Hoving, and P. Grünberg, Phys. Rev. Lett. **67**, 903 (1991).

[17] J. Zak, E. R. Moog, C. Liu, and S. D. Bader, J. Magn. Magn. Mater. **89**, 107 (1990).

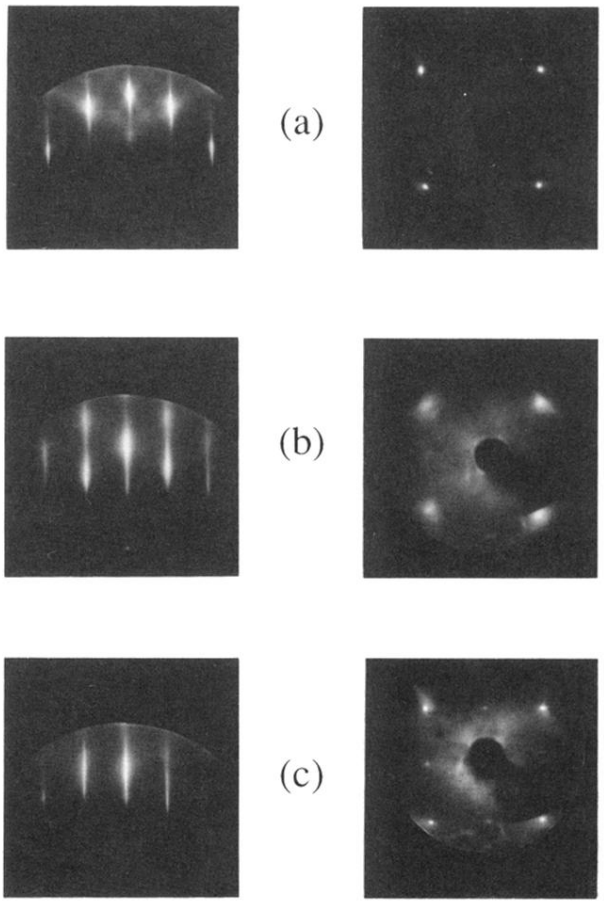

FIG. 1. The RHEED (left) and LEED (right) patterns for (a) the Ag(100) substrate; (b) 6 ML of Fe on Ag(100); and (c) after annealing of the film in (b) at 150 °C. The electron energy of the LEED pictures is ~120 eV.